

# CHAPTER 5

## YOUNG ALKALI-BASALT FROM JAPAN TRENCH

### 5-1 Introduction

During the ROV *KAIKO* mission to the Japan Trench area, cruise KR97-11 of Japan Marine Science and Technology Center (JAMSTEC), continuous outcrops of alkaline pillow basalt were documented and sampled at the oceanward slope toe of the northern Japan Trench at around 7325 to 7360 m depth. The slope is characterized by trench-parallel (N-S) normal faults with some NNW or NNE faults, due to the warping of the down-going Pacific Plate of the Early Cretaceous age (Kobayashi *et al.*, 1998) (Figure 2.2). These normal faults bound horst and graben structures that are approximately 5 km in horizontal extent with 100 m to 500 m scale vertical separations (Ogawa *et al.*, 1996; Ogawa and Kobayashi, 1993). There is no distinct seamount topography associated with the alkaline pillow basalt outcrops, however an indistinct mound-like feature (100 to 200 m height, 1 to 2 km in diameter) is recognized using Sea Beam sonar bathymetric mapping (Figure 2.3).

Alkali-basalts occur in various parts on the surface of the earth, most particularly in the continental and hotspot areas. Such occurrences have been known as products of deep-origin magma from the upper mantle or further depths. However, peculiar occurrences of a kind of alkali-basalt have been known in some limited oceanic

areas, and in most cases the places of eruptions are related to tectonically interesting positions, such as along deep fractures of oceanic crust.

The ROV *KAIKO* was used to map and sample to the toe of the oceanward slope of the downgoing Pacific Plate slab of the northern Japan Trench of approximately 7300 to 7400 meters depth at around  $39^{\circ} 23' N$ ,  $144^{\circ} 16' E$ . The slopes have an average dip of  $25^{\circ}$  but are locally very steep, exposing alkaline pillow basalt outcrops at depths of 7325 to 7360 m. The cliffs are covered with only thin draping of soft, black, muddy sediments. The total thickness of the basalt outcrops is more than 35 m. The outcrops are alternations of pillow lava and hyaloclastite (Figure 5.1).

This study tries to expect an origin of such curious alkali-basalts from the Ar-Ar geochronology, petrology and geochemistry.

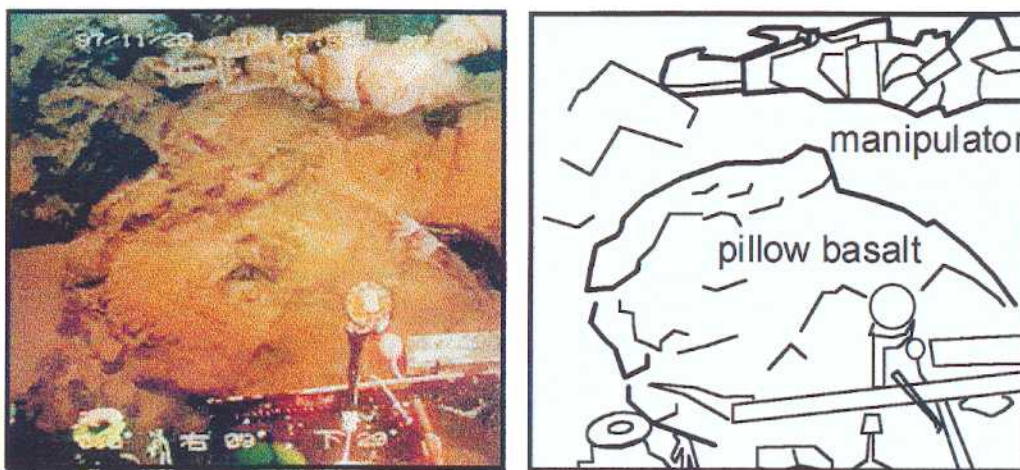


**Figure 5.1** Photograph and sketch of alkali-basalt outcrop at Japan Trench oceanward slope. Around here, pillow basalt, hyaloclastite and muddy black sediments are dominated.

## 5-2 Results

Two samples, 10K#56 R-001 and R-002, were collected from the pillow lava outcrops at around 7360 m depth. Both samples have a curved foliation, representing a surface of the pillow of around 30 cm in diameter. The samples contain a large proportion of vesicles, reaching a maximum of 40 volume percent.

### *Bulk Geochemistry*

Bulk chemical compositions (Table 5.1 and 5.2) show the potassium-rich alkali-basalt, shoshonite, or slightly differentiated, mugearite, and characterize that these rocks are rich in more incompatible elements. Groundmass excluded olivine phenocrysts which are probably xenocrysts (described the next) were also analyzed.

**Table 5.1** Results of XRF analysis of bulk and groundmass chemistry of 10K#56 R001 and R002. Groundmass is the matter of excluding the olivine phenocryst by the magnetic separator.

Japan Trench oceanward slope				
10K#56	R-001	R-001	R-002	R-002
	bulk	groundmass	bulk	groundmass
wt%				
SiO <sub>2</sub>	48.22	48.84	48.45	49.27
TiO <sub>2</sub>	2.56	2.72	2.84	2.84
Al <sub>2</sub> O <sub>3</sub>	10.30	11.60	11.26	12.18
Fe <sub>2</sub> O <sub>3</sub>	6.38	10.44	6.12	10.00
FeO	4.23	-	4.36	-
MnO	0.14	0.13	0.13	0.12
MgO	11.68	8.23	7.83	6.61
CaO	7.47	7.68	8.14	7.61
Na <sub>2</sub> O	2.95	3.04	3.28	3.13
K <sub>2</sub> O	3.17	3.88	3.63	4.11
P <sub>2</sub> O <sub>5</sub>	0.78	0.83	0.84	0.87
H <sub>2</sub> O+	1.76	1.23	2.49	1.47
H <sub>2</sub> O-	0.36	1.39	0.64	1.81
Total	100.00	100.00	100.00	100.00
ppm				
Ba	1202.3	1176.8	1209.5	1191.2
Ce	94.4	-	108.7	-
Co	56.7	154.0	46.7	129.0
Cr	527.8	424.0	400.5	353.0
Ga	17.7	-	20.2	-
Nb	36.6	37.4	40.3	39.4
Ni	418.1	163.1	227.8	117.2
Pb	7.2	6.9	7.3	7.3
Rb	47.0	56.2	53.1	59.0
Sr	1076.5	1212.4	1092.4	1140.4
Th	2.0	4.7	2.0	4.9
V	140.1	-	143.4	-
Y	14.2	18.8	15.3	19.7
Zr	243.0	263.8	259.9	273.8

Table 5.2 Results of ICPMS analysis of bulk chemistry of 10K#56 R001 and R002.

10K#56	R-001 bulk	R-002 bulk
ppm		
Y	19.17	20.78
La	54.07	58.69
Ce	106.95	114.28
Pr	12.03	12.97
Nd	49.35	53.61
Sm	9.41	10.02
Eu	2.98	3.22
Gd	7.74	8.38
Tb	1.00	1.08
Dy	4.63	4.72
Ho	0.77	0.88
Er	1.83	1.93
Tm	0.23	0.23
Yb	1.41	1.46
Lu	0.19	0.20

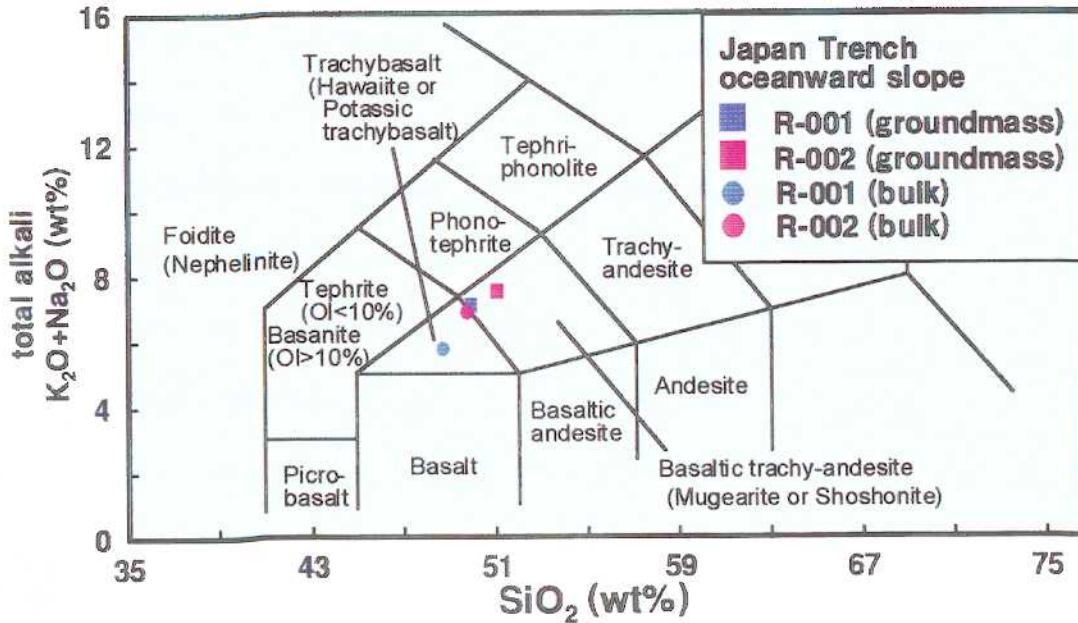


Figure 5.2 SiO<sub>2</sub>-total alkali diagrams of 10K#56R-001 and R-002 from Japan Trench oceanward slope.

## *Mineralogy*

The rocks have almost the remarkable quench texture and mineral composition and are very fresh without any altered minerals, even in vesicles. Large olivine phenocrysts attain 1.0 % in R-001 in volume and 2.4 % in R-002 and the groundmass is composed of olivine, Ti-augite, microcline and opaque minerals as primary minerals.

The olivine phenocrysts (high Fo values, 90-93, and NiO contents, 0.3-0.5 wt%) (Figure. 3B) are more primitive in origin than those in the groundmass (high Fo values, 80-90, and NiO contents, 0.1-0.5 wt%), and have the compositions of equilibrium with mantle olivine array (Sato, 1977; Takahashi *et al.*, 1987) (Figure 5.3).

Low Si Ti-augite (Figure 5.4) and many opaque minerals in the groundmass characterize mineral compositions of these rocks. Two diagrams of clinopyroxene are plots of SiO<sub>2</sub> vs. Al<sub>2</sub>O<sub>3</sub> and Al(z) vs. TiO<sub>2</sub> after LeBas (1962) (Figure 5.4). Al(z) is the percentage of tetrahedral sites occupied by Al. The nonalkaline/alkaline and alkaline/peralkaline boundaries on these diagrams were determined from groundmass compositions LeBas (1962). Two effects from magma chemistry are observed on the two plots; (1) The silica-saturation of a magma controls the amount of tetrahedral aluminum substitution. Titanium positively correlates with Al(z) because of the cation charge deficit in the tetrahedral sites (Al<sup>3+</sup> vs. Si<sup>4+</sup>), (2) Differentiation derives clinopyroxene compositions to lower Al(z) and higher Ti for tholeiite (nonalkaline) liquids and to higher Al(z) and higher Ti for alkaline liquids.

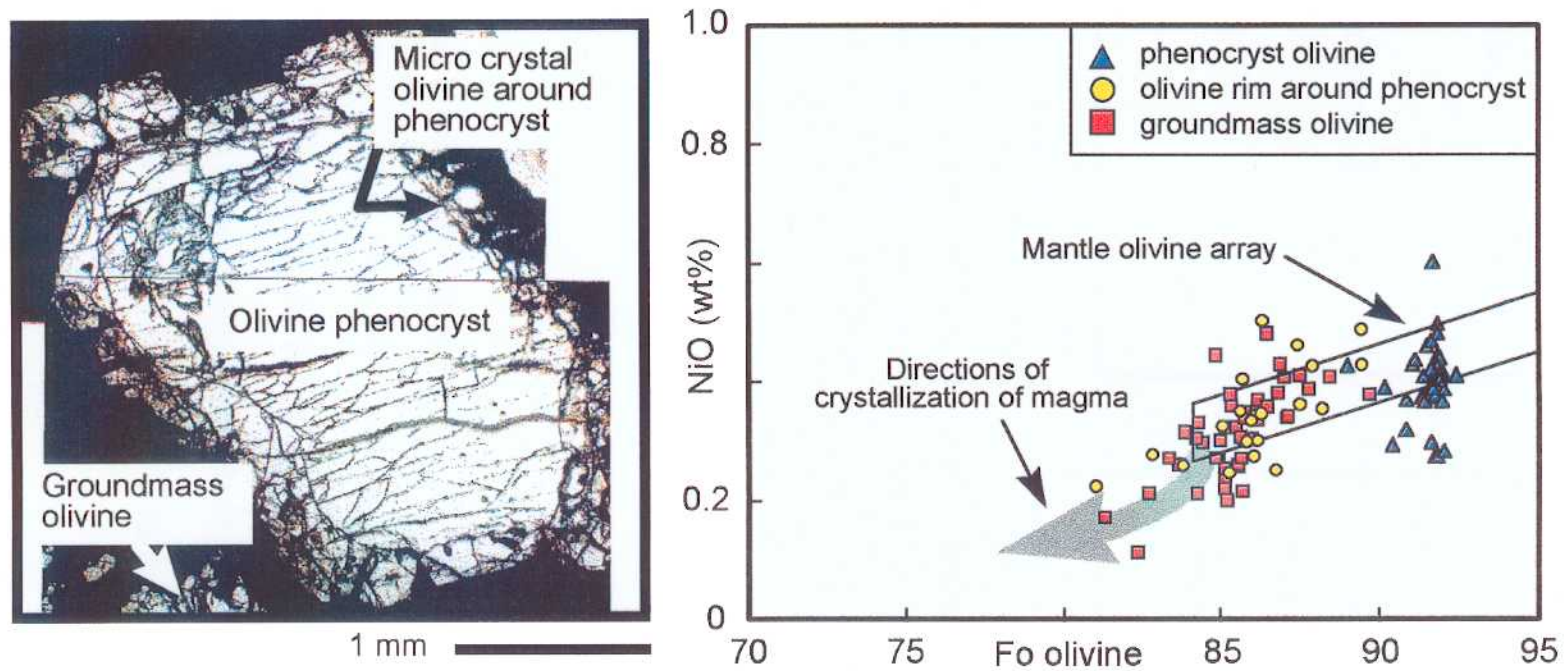


**Figure 5.3** Photomicrograph of thin section of various olivines in the 10K#56R2 and Fo value vs. NiO plot of various olivines. Open box zone is mantle olivine array after Takahashi *et al.* (1987). An arrow show the trend of olivine fractional crystallization after Sato (1977).

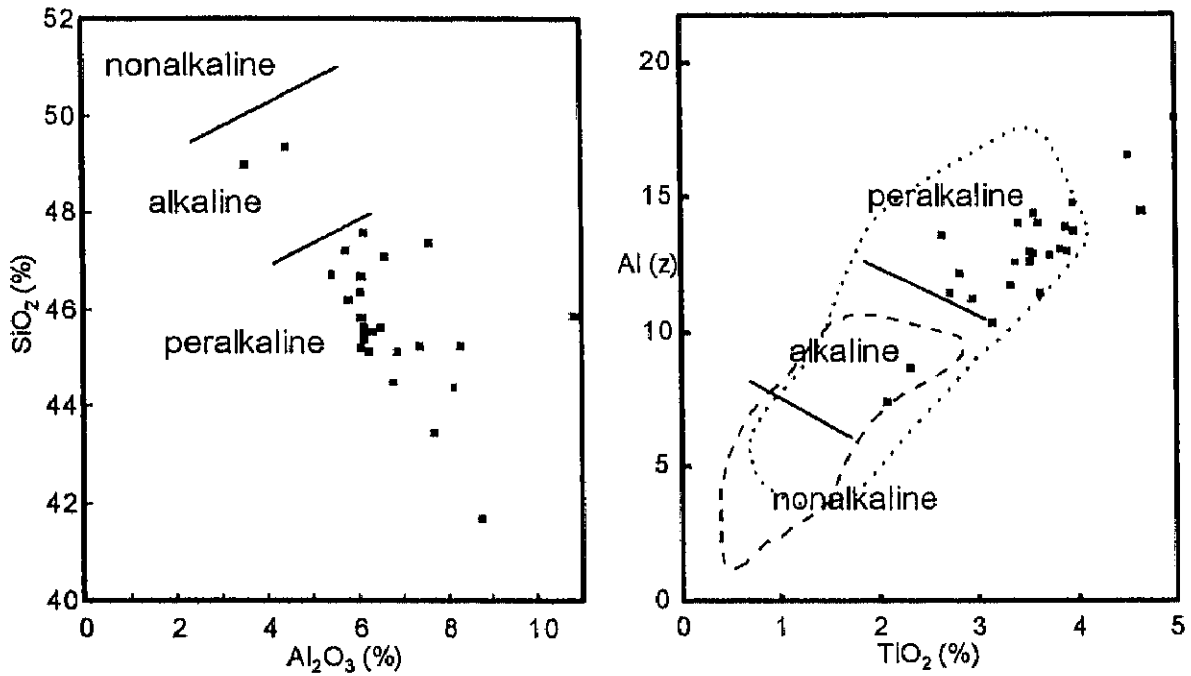


**Figure 5.4** SiO<sub>2</sub> vs. TiO<sub>2</sub> and Al(z) vs. TiO<sub>2</sub> plots of clinopyroxene. Divisions between nonalkaline/ alkaline/ peralkaline fields documented by Le Bas (1962). Al(z) is after Le Bas (1962) for groundmass compositions.

### *Ar-Ar Age*

A good plateau age,  $5.95 \pm 0.31$  Ma, for 10K#56 R-002 bulk rock are calculated in the age spectrum (Figure 5.5). The error of the J-value was not used in age spectrum, and will be included at the last stage of age calibration as a plateau age. In addition, we can obtain a considerably well-defined isochron in the inverse isochron (Figure. 5.5b), and an isochron age,  $5.69 \pm 0.43$  Ma, agrees with the plateau age.



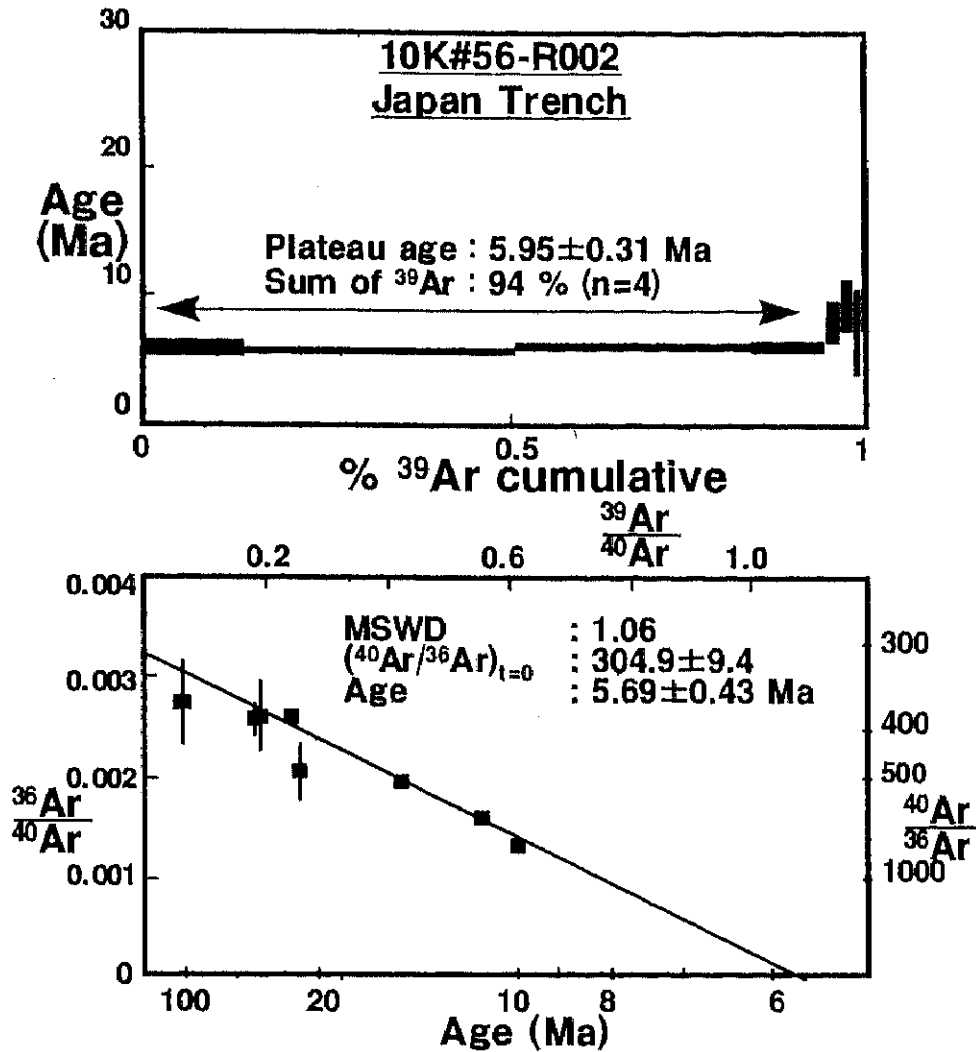


**Figure 5.5** Ar-Ar age result of 10K#56-R002 from Japan Trench oceanward slope. Age spectra and isochron diagrams for  $^{40}\text{Ar}/^{39}\text{Ar}$  incremental heating experiments on 10K#56R-002 shoshonite. We used a J value;  $J = (3.412 \pm 0.063) \times 10^{-3}$ , which define a dimensionless parameter determined for each irradiation from standard samples whose ages are known from conventional potassium-argon measurements (Mitchell, 1968). Standard samples are three "HD-B1 biotite ( $24.0 \pm 0.4$  Ma)". The correction factors for the interfering isotopes during the irradiation of samples were determined experimentally as follows;  $(^{36}\text{Ar}/^{37}\text{Ar})_{\text{ca}} = (3.744 \pm 0.082) \times 10^{-4}$ ,  $(^{39}\text{Ar}/^{37}\text{Ar})_{\text{ca}} = (9.30 \pm 0.44) \times 10^{-4}$ . The mean squared weighted deviations,  $\text{MSWD} = \text{SUMS}/(n-2)$  (York, 1969), indicates how well data fit the least-squares calculated straight line in the three isotope diagram.

### 5-3 Discovery of Young Basalts

Small seamount volcanoes are well-known from the present day Pacific ocean floor. Floyed (1991) demonstrates that many small seamounts decorating the Pacific lithosphere were built up shortly after ridge magmatism. Although these small seamounts are only known from bathymetric studies, alkaline basalt in this study will have different origins with those of Floyed (1991), because the present alkaline basalt is very young, much younger than the ocean floor around this area. In addition, there are rather many seamounts and guyots just off the Japan trench, as the Joban Seamount Chain (Masalu *et al.*, 1997; Nakanishi *et al.*, 1998 etc.), and the Erimo and Takuyo seamounts (Figure 2.2). The representative 120 Ma Daiichi-Kashima Seamount and 104 Ma Erimo Seamount are known (Takigami *et al.*, 1989), and they must be the products of hotspot origin because of the petrological characteristics and the straight distributions. Notwithstanding that these seamounts are all of Cretaceous age, the present rocks are 6 to 8 Ma in age, late Miocene, and are of very small volume amount. The seafloor topography does not show any edifice for a large seamount but only a small (Figure 2.3). In addition, we do not have any hotspot even though tracing back the present Pacific plate motion to those ages.

Mineral characteristics and trace element bulk compositions are similar to the undifferentiated post-shield rejuvenated volcanism in Hawaii and Samoa, which are known as eruptions of strongly alkaline lavas after passing on the hotspot (Nakamura, 1986; Hawkins and Natland 1975; Natland, 1980). Alkaline basalt in this study is similar to these lavas in the points of large primitive olivine xenocrysts, high Al(z) and low Si clinopyroxene (Ti-augite), and mineral association. However, the major elements bulk compositions are more differentiated (48 to 50 wt% SiO<sub>2</sub>) than nephelinite and

basanite. In both areas of Hawaii and Samoa, the post-shield volcanisms are thought to erupt along ruptures in the oceanic lithosphere, which may be originated from tensional cooling after passing the hotspot (Nakamura, 1986) or from rupturing by deformation of the oceanic lithosphere (Hawkins and Natland, 1975; Natland, 1980).

When we trace back the present position using the present "absolute" motion of the Pacific plate, 10.29 cm/yr to 295.26 degrees (Gripp and Gordon, 1990), we obtain the 6 Ma position to be between approximately 600 km ESE off the northern Japan Trench. Asking the bathymetric chart of the northwest Pacific, this area corresponds not to the outer buldge (Hokkaido Rise; Figure 2.2) but to the deepest portion of the Pacific plate just before the bulge (Figure 5.6). If a fracture occurs or rejuvenated in the oceanic lithosphere, magma which exists at the lowest boundary approximately 100 km depth. The occurrence, mineralogical and chemical characteristics of the basalt could explain the setting.

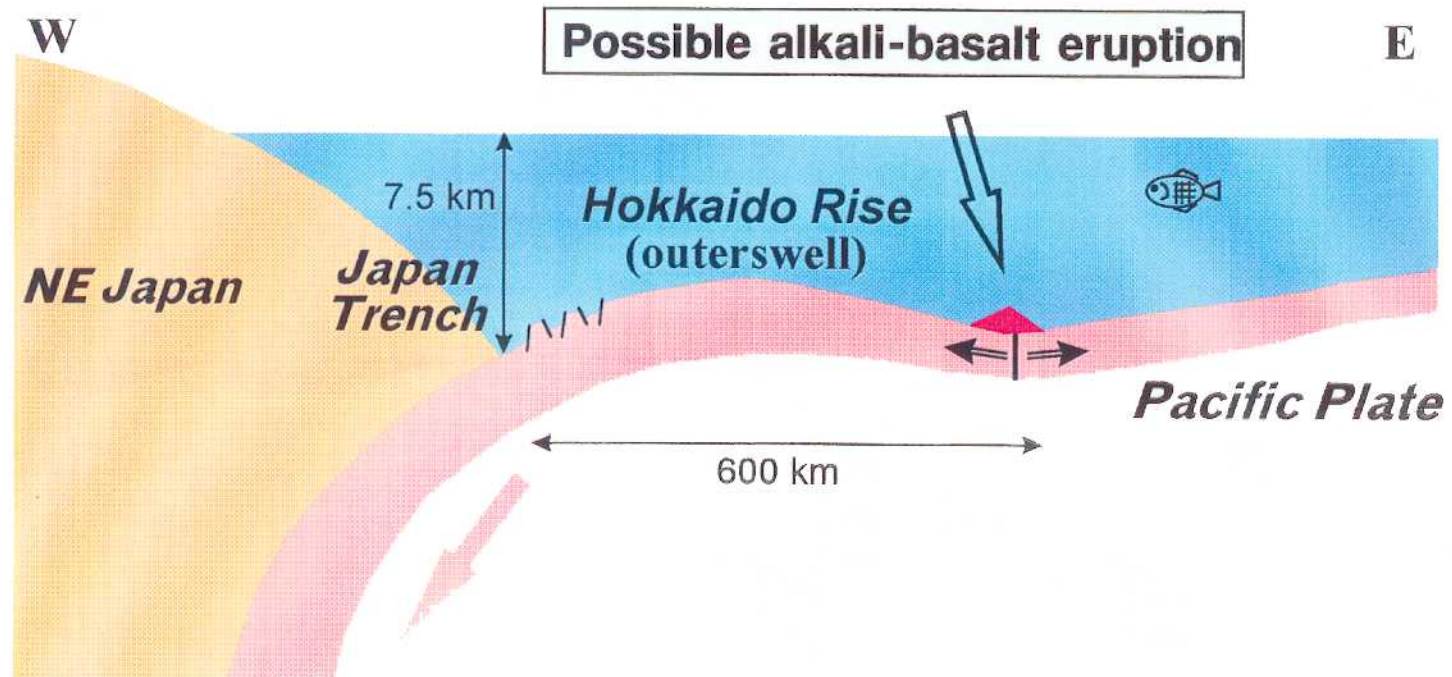


Figure 5.6 The model of possible alkali-basalt eruption on the old oceanic crust toward the subduction zone.